Carpathian Journal of Earth and Environmental Sciences, November 2013, Vol. 8, No. 4, p. 139 - 146

RHODOCHROSITE-BEARING CONCRETIONS FROM A JURASSIC MANGANESE ORE MINERALIZATION – ÚRKÚT, HUNGARY

[1]Márta POLGÁRI, [2]Lóránt BÍRÓ, [2]Elemér PÁL-MOLNÁR, [1]Gábor DOBOSI, [1]Bernadett BAJNÓCZI, [1]Tibor NÉMETH, [3]Viktória KOVÁCS KIS & [4]Tamás VIGH

[1]Institute for Geological and Geochemical Research, Research Centre for Astronomy and Earth Sciences, Hungarian Academy of Sciences, corresponding author: M. Polgári, e-mail: rodokrozit@gmail.com, Tel/Fax: +36 1 319-3137
[2]Szeged University, Dept. of Mineralogy, Geochemistry and Petrology, 6702 Szeged, Egyetem str. 2-6, Hungary
[3]Research Institute for Technical Physics and Materials Science, Research Centre for Natural Sciences, Hungarian Academy of Sciences, H-1121 Budapest, Konkoly Thege M. út 29-33., Hungary
[4]Mangán Ltd., H-8409, Úrkút, Hungary

Abstract: Rhodochrosite concretions with fish and plant fossils occur in the Úrkút manganese carbonate deposit (Jurassic) and were investigated for mineralogy and geochemistry. These concretions are mainly composed of rhodochrosite and Mn-bearing calcite, but X-ray diffraction and electron microprobe analysis showed also the presence of Ca-rich kutnohorite. Cathodoluminescence microscopy revealed kutnohorite as luminescent mineral as infiltration and veinlets suggesting early diagenetic origin. Chrysotile needles were also detected in one of the kutnohorite veinlets by transmission electron microscopy. Stable C and O isotope results showed low-T very early diagenetic, bacterially mediated decomposition of organic matter and formation of Mn-carbonate in the ore section, which effect was the strongest around the organic remnants. Compared to the polarized light microscopy, cathodoluminescence microscopy was able to give visible picture about the texture of the very fine-grained Mn-carbonate concretions; therefore it was proved to be a useful method in study of diagenetic processes in manganese deposits.

Keywords: kutnohorite, chrysotile, concretion, fish, manganese, Jurassic, Hungary

1. INTRODUCTION

Carbonate concretions on methane seeps are usually forming at local concentrations of organic matter an origin by anaerobic CH_4 oxidation (Lash & Blood, 2004; Buggish & Krumm, 2005). Concretions formed around organic fragments are common, among them fish-bearing ones (Fara et al., 2005; El et al., 2002). Ca-phosphate concretions around the organic remnants up to 31 wt.% P_2O_5 content also occur (Tarawneh & Moumani, 2006). Isotope geochemistry (C, O, S) delineate the origin and the associated diagenetic environment for the formation of concretions via sulphate reduction, and methanogenic zones (Woo & Khim, 2006).

Concretions of variable size and colour (10-50 cm in diameter; light grey, brown, pink) are also common in the black shale-hosted Mn-carbonate deposit of Jurassic (Toarcian) at Úrkút basin, Hungary (Úrkút Manganese Formation - ÚMnF). The concretions generally contain coalified or silicified plant fragments or fish fossils (Polgári et al., 2000, 2005).

The fish fossils can give information about the conditions of manganese ore formation. Recently, a new genetic model was proposed for the Mn deposit according to which two cycles of bacterial activity took place during ore formation. Cycle 1 was a near-seabed aerobic chemolithoautotroph cycle that was essential in sequestering metal ions (Mn^{2+}, Fe^{2+}) from solution via enzymatic Mn(II) oxidation. Mn-oxide proto-ore was deposited in the sediment pile, serving as a paleoenvironmental indicator of oxic conditions. Cycle 2 was an anaerobic/suboxic heterotrophic bacterial cycle in which early diagenetic bacterially mediated Mn(IV) and Mn(III) reduction processes took place via organic matter oxidation and Mn-carbonate mineralization (Polgári et al., 1991, 2012). For the source of metals low-temperature fluid flow along an associated fracture

zone is preferred (Polgári et al., 2012). It is known from the early 1930s that the Mn-carbonate ore and black shale contains high amount of microscopic fish remnants and rarely well-preserved whole fish fossils that were found in concretions in some layers of the sediments' pile. The large amount of fish debris can increase the P_2O_5 content of the ore up to 16 wt. % in some layers, mainly in the second Mn-carbonate ore bed. The concretions were thought to consist of phosphorite. During the mining activity about 12-15 fish fossils were found in light brown, pink, hard concretions. The determination of two fish fossils as *Caturus sp* and *Eomesodon sp* have been made by Pászti (2004).

The aim of the present study is to give a summary on the mineralogy of concretions and a detailed geochemical characterization of four representative fish-bearing concretions to get more information about their formation conditions. We are going to show an example of sedimentary-diagenetic cold temperature formation of kutnohorite and chrysotile via bacterially mediated manganese ore formation and diagenesis.

2. GEOLOGICAL SETTING

The Mn deposits embedded in sedimentary rocks are located at Úrkút-Csárda Hill in the central Bakony Mountains (Transdanubia), in the North Pannonian unit of the Alps-Carpathians-Pannonian (ALCAPA) region (Fig. 1). The Transdanubian Range as a part of the Periadriatic region of the Southern Alps is an allochthonous domain, which escaped north-eastward from the continental convergence (collision) zone between Africa (Apulian microplate) and Europe (Kázmér & Kovács, 1985).

The largest Mn mineralization (70 million tons of Mn ore with 14 million tons of metal content) occur in the Úrkút basin, which were formed by the NW–SE trending block faulting that characterized the Late Triassic and the Jurassic of this region. The deposits are Early Jurassic (Late Lias) and are within marine sedimentary rocks composed mainly of bioclastic limestone, radiolarian clay marlstone and dark-grey to black shale (Polgári et al., 2000). In the Tethyan Realm, Jurassic was an important epoch of Mn mineralization; Mn deposits with variable reserves and Mn-bearing cherts are distributed from S–Spain to Greece and Oman.

3. SAMPLES AND METHODS

22 concretions were collected from the Úrkút Manganese Mine (shaft No. III. +186 level) Transdanubia, Hungary (Fig. 2) and examined by X-ray powder diffraction (XRD) for mineralogy and stable C and O isotope distribution (sample numbers: KK001-019, ORG3, 134). Four selected, representative fish-bearing concretions (H1-4) were analyzed in detail by polarizing and cathodoluminescence (CL) microscopy complemented by transmission electron microscopy (TEM), and SEM-EDS.

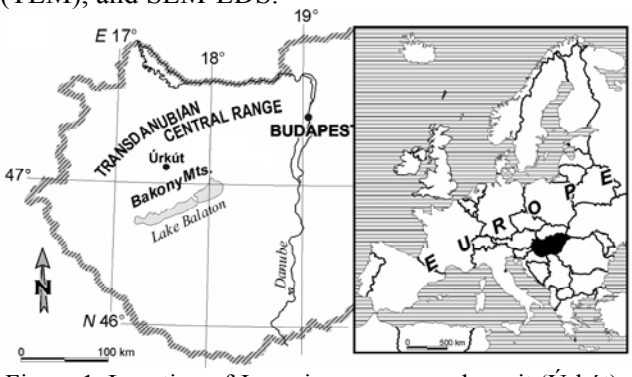

Figure 1. Location of Jurassic manganese deposit (Úrkút) in the central Bakony Mountains (Transdanubia), North Pannonian Unit, Alps-Carpathians-Pannonian (ALCAPA) region. Black shale sedimentation was involved in the area of Úrkút in Early Toarcian (Vörös & Galácz, 1998).

The elongated or spherical, egg-like concretions are hard, fine-grained, light-dark brown, pinkish, and inside they are inhomogeneous or concentric. Around fossils they are darker and toward the outer part lighter (dark part-core; medium; light part-marginal part; Table 1). The diameter of the concretions is up to 30-50 cm. Rarely, veinlets of a few mm wide cut the matrix of the concretions.

Mineralogical composition of all samples were analysed by routine X-ray powder diffraction. Philips 1730 X-ray diffractometer with a graphite crystal monochromator and CuK_α radiation was used and continuous scans were run from 3-70° 2Θ at 45 kV and 35 mA, yielding a scan speed of 0.02° 2Θ/s.

Cathodoluminescence (CL) examinations were performed on polished rocks chips and thin sections of fish-bearing samples (H1-4) using a Reliotron „cold-cathode" equipment mounted on a Nikon E600 microscope and operated at 5-7 kV accelerating voltage and 0.9 mA current.

Quantitative SEM-EDS measurements of carbonates were performed on the carbon-coated chips of fish-bearing samples using a JEOL Superprobe 733 microprobe equipped with Oxford INCA 2000 energy-dispersive X-ray spectrometer (EDS). Analytical conditions were 15 kV accelerating voltage, 5 nA beam current and a count time of 50 s. Calcite, dolomite, siderite and spessartine (for Mn) standards were used for calibration.

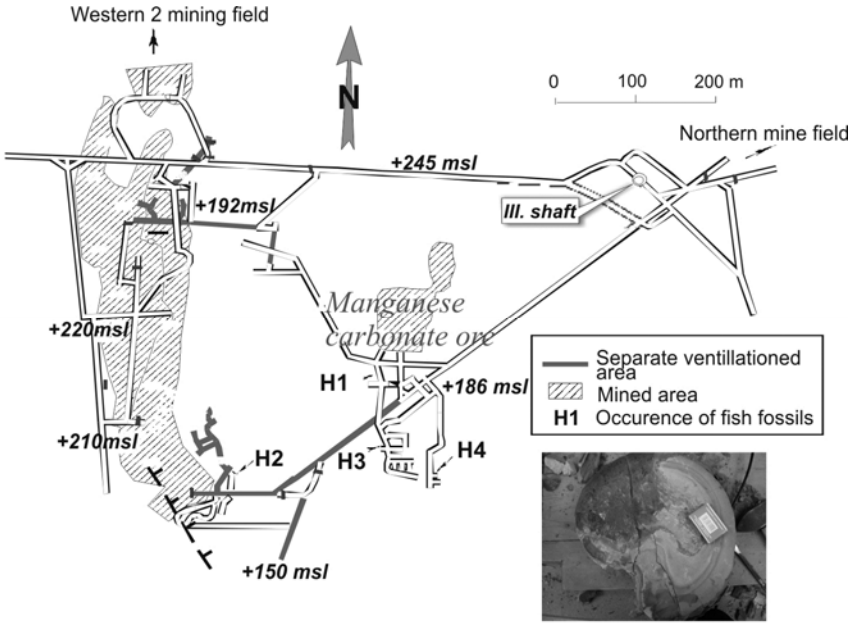

Figure 2. Location of the Úrkút Manganese Mine in Hungary, sampling in the mine, and concretion H1

An alternative calibration using wollastonite, MgO, haematite and spessartine standards gave practically the same results. All analyses were made using fast scanning mode at different magnifications to prevent carbonate decomposition under the electron beam and in case of very fine scale of inhomogeneity to produce average value for the analysed area.

A fragment from the luminescent veinlet of H4 sample was gently crushed in ethanol and a drop of the resulted suspension was deposited onto a copper grid covered by lacy carbon supporting film for TEM.

Table 1. Mineralogy of concretions occurred in the black shale-hosted Mn-carbonate deposit, Úrkút, Hungary

Sample code	Sample phase (number of concretions)	Mineral composition		
		Main	Moderate	Rare
KK1-19, ORG3, 134 concretions	bulk (11)	rhodochrosite (Ca-, Mg-bearing)	Mn-bearing calcite	smectite, quartz, fedspar, apatite, barite,
	bulk (6)	Mn-bearing calcite	rhodochrosite (Ca-, Mg-bearing)	smectite, kutnohorite, quartz, fedspar, apatite, barite,
	bulk (1)	quartz	calcite, rhodochrosite, dolomite	pyrite
Selected, representative fish-bearing concretions "fish balls"				
H1	dark part	rhodochrosite	hydroxyl-apatite	
H1	bulk	rhodochrosite	kutnohorite	smectite
H2	dark part	quartz	hydroxyl-apatite	
H2	bulk	quartz, cristobalite	rhodochrosite	
H3	bulk	rhodochrosite	smectite	kutnohorite
H4	bulk	rhodochrosite	kutnohorite	

The TEM images were obtained with a Philips CM20 electron microscope operating at 200 keV. The composition of the carbonate was measured using a NORAN energy dispersive X-ray spectrometer.

Stable C and O isotope study was made on the bulk material of the concretions (18 samples) and from layer to layer a detailed study was carried on "fish balls" by a Finnigan MAT delta S isotope ratio mass spectrometer by routine methods. Three sample preparation ways were used and data compared on most of the samples (2 days frozen period + 20 mg sample; 3 days frozen period and 30 mg sample; and 2 days frozen period and 30 mg sample using diluted phosphoric acid). 12 samples were tested by two of these methods, and the results did not show characteristic differences, that is why the average data were used.

4. RESULTS

4.1. Mineralogy

The main minerals of the concretions are rhodochrosite, Mn-bearing calcite with traces of hydroxyl-apatite, kutnohorite, smectite, quartz, feldspar, barite, pyrite, and in one sample (H2) quartz-cristobalite. Hydroxyl-apatite was characteristic near the fish fossils (Table 1).

4.2. Chemistry

Backscattered electron images revealed that the bulk material of "fish balls" is a mixture of two phases, rhodochrosite and kutnohorite. Irregularly shaped light and dark patches alternate in the sample, the size of the patches as well as the proportion of the two phases, changes from site to site. The dark veinlet in sample H4 exhibits apparently homogenous appearance. The two phases occur with different and well-defined composition in μm scale distribution. The average areal chemical composition is the mixture of the two types of carbonate phases on different rate. The compositions of the samples according to the different colored parts (light, medium and dark) are in Table 2. The CaO content of the concretions varies between a few to 20 wt. % in all zones. The marginal part of H4 concretion shows Ca enrichment up to 39.89 wt. % (Table 2). The core of H1 and H2 concretions show phosphate $Ca_5((PO_4)_3$ enrichment around the fish fossils (from a few to 15.1 wt. % P_2O_5 content, Table 2).

H1 and H4 concretions are SiO_2 poor in all their three zones. Concretion H2 is very SiO_2- and Ca-rich in the core (52.74 and 18.06 wt. %) and towards the margin the Ca content decreases to a few wt. %, while the SiO_2 is around 69.32 wt. % with a maximum (94.04 wt.%) in the medium zone.

Concretion H3 shows elevated Ca content in the core (18.49 wt. %) which decreases to 2.80 wt. % in the medium zone and increases again to 10.27 wt. % in the marginal zone. Its SiO_2 content is only a few % in the core but increases to 29.43 wt. % in the medium zone.

Other elements (Al, Fe, Mg) occur in a few wt.% (Table 2) as substituting Mn or Ca carbonate and in a clay mineral. Phosphate-rich parts close to the fish fossils are well distinguishable. The Ca-Mn correlation shows well-determined negative correlation between the two elements. Si-Mn relations show negative tendencies and strong silification of Mn-rich parts.

Table 2. Chemical composition of fish-bearing concretions (Úrkút Manganese Mine) by EDX in wt. % in oxide form

Sample code and part	**SiO_2**	**TiO_2**	**Al_2O_3**	**FeO**	**MnO**	**MgO**	**CaO_{tot}**	**CaO_{phos}**	**Na_2O**	**K_2O**	**P_2O_5**
H1 part 1	0.11	0.00	0.09	0.41	40.26	0.00	13.94	3.93	0.70	0.05	9.94
H1 part 1	0.20	0.00	0.11	0.36	41.36	0.19	12.14	3.12	0.30	0.04	7.90
H1 part 1	0.00	0.00	0.00	0.00	39.35	0.28	12.73	3.52	0.00	0.01	8.91
H1 part 1	0.34	0.00	0.17	0.52	41.62	0.43	12.60	3.22	0.24	0.00	8.14
H1 part 1 average (dark)*	**0.16**	**0.00**	**0.09**	**0.32**	**40.65**	**0.23**	**12.85**	**3.45**	**0.31**	**0.03**	**8.72**
H1 part 2	0.92	0.09	0.36	0.60	43.78	1.04	8.94	0.14	0.00	0.22	0.35
H1 part 2	0.43	0.04	0.15	0.17	41.95	1.10	12.11	0.09	0.17	0.02	0.24
H1 part 2	0.37	0.18	0.20	0.51	42.89	1.04	10.79	0.11	0.21	0.00	0.27
H1 part 2	0.89	0.03	0.90	0.00	43.05	1.02	8.93	0.19	0.08	0.00	0.49
H1 **part 2 average (medium)**	**0.65**	**0.09**	**0.40**	**0.32**	**42.92**	**1.05**	**10.19**	**0.13**	**0.12**	**0.06**	**0.34**
H1 part 3	1.92	0.00	1.04	0.29	32.03	2.06	19.25	0.15	0.16	-0.02	0.38
H1 part 3	2.35	0.00	0.61	0.03	30.74	2.08	21.09	0.12	0.00	0.01	0.30
H1 part 3	1.56	0.00	0.83	0.11	34.88	2.21	17.07	0.06	0.07	0.08	0.15
H1 part 3	1.40	0.04	0.52	0.21	31.99	1.70	20.31	0.25	0.00	-0.03	0.64
H1 part 3 average (light)	**1.81**	**0.01**	**0.75**	**0.16**	**32.41**	**2.01**	**19.43**	**0.15**	**0.06**	**0.01**	**0.37**
H2 part 1	55.25	0.00	0.12	0.07	6.56	0.16	16.75	5.33	0.55	0.04	13.48
H2 part 1	50.70	0.00	0.18	0.00	5.26	0.00	20.31	6.51	0.34	0.00	16.48
H2 part 1	53.32	0.17	0.08	0.14	7.75	0.18	16.57	5.74	0.51	0.04	14.54
H2 part 1	51.69	0.00	0.41	0.00	6.33	0.08	18.62	6.29	0.40	0.00	15.91
H2 part 1 average (dark)	**52.74**	**0.04**	**0.20**	**0.05**	**6.48**	**0.11**	**18.06**	**5.97**	**0.45**	**0.02**	**15.10**
H2 part 2	94.53	0.08	0.43	0.00	1.18	0.17	0.00	0.00	0.12	0.05	0.00
H2 part 2	93.54	0.03	0.31	0.03	1.35	0.00	0.28	0.00	0.08	0.14	0.00
H2 part 2 average (medium)	**94.04**	**0.06**	**0.37**	**0.02**	**1.27**	**0.09**	**0.14**	**0.00**	**0.10**	**0.10**	**0.00**
H2 part 3	70.87	0.10	0.55	0.17	15.76	0.51	1.22	0.07	0.36	0.04	0.18
H2 part 3	71.08	0.10	0.17	0.11	16.53	0.61	1.24	0.13	0.01	0.05	0.33
H2 part 3	67.17	0.00	0.28	0.00	19.46	0.13	1.22	0.10	0.00	0.14	0.25
H2 part 3	68.17	0.00	0.83	0.00	18.36	0.28	1.35	0.15	0.04	0.06	0.38
H2 part 3 average (light)	**69.32**	**0.05**	**0.46**	**0.07**	**17.53**	**0.38**	**1.26**	**0.11**	**0.10**	**0.07**	**0.29**
H3 part 1	0.90	0.03	0.08	0.00	33.62	1.57	19.20	0.00	0.00	0.01	0.00

Sample code and part	SiO_2	TiO_2	Al_2O_3	FeO	MnO	MgO	CaO_{tot}	CaO_{phos}	Na_2O	K_2O	P_2O_5
H3 part 1	0.92	0.00	0.49	0.53	33.61	1.97	19.20	0.06	0.03	0.00	0.14
H3 part 1	2.06	0.03	0.27	0.21	33.75	1.77	18.00	0.12	0.11	0.04	0.31
H3 part 1	1.00	0.11	0.41	0.20	34.30	1.72	17.57	0.13	0.18	0.07	0.32
H3 part 1 average (bright grey)	**1.22**	**0.04**	**0.31**	**0.24**	**33.82**	**1.76**	**18.49**	**0.08**	**0.08**	**0.03**	**0.19**
H3 part 2	30.34	0.00	2.68	2.04	23.17	12.65	2.78	0.08	0.33	0.60	0.20
H3 part 2	28.13	0.15	2.15	2.33	24.11	12.03	2.82	0.02	0.00	0.62	0.04
H3 part 2	28.81	0.23	2.92	2.21	24.46	11.23	2.58	0.00	0.12	0.67	0.01
H3 part 2	30.85	0.18	2.79	2.70	22.07	13.23	2.74	0.00	0.07	0.73	0.00
H3 part 2	29.01	0.08	2.46	1.94	23.66	12.30	3.07	0.07	0.03	0.46	0.17
H3 part 2 average (grey)	**29.43**	**0.13**	**2.60**	**2.24**	**23.49**	**12.29**	**2.80**	**0.03**	**0.11**	**0.62**	**0.08**
H3 part 3	8.39	0.28	0.93	0.50	34.08	4.98	11.61	0.04	0.17	0.16	0.10
H3 part 3	13.54	0.00	1.21	0.45	33.21	8.28	9.23	0.14	0.16	0.14	0.35
H3 part 3	14.29	0.05	1.23	0.64	32.38	7.29	7.78	0.02	0.01	0.46	0.06
H3 part 3	8.79	0.00	0.68	0.59	33.78	4.90	12.47	0.00	0.19	0.10	0.01
H3 part 3 average (light)	**11.25**	**0.08**	**1.01**	**0.55**	**33.36**	**6.36**	**10.27**	**0.05**	**0.13**	**0.22**	**0.13**
H4 part 1	1.84	0.13	4.66	0.14	43.43	1.85	5.18	0.06	0.14	0.03	0.15
H4 part 1	1.64	0.00	4.55	0.03	42.86	1.97	5.07	0.17	0.30	0.12	0.43
H4 part 1	1.50	0.02	4.67	0.59	43.27	1.37	5.21	0.21	0.23	0.07	0.54
H4 part 1	1.31	0.03	4.72	0.00	44.51	1.58	5.18	0.28	0.15	0.00	0.70
H4 part 1 average (light)	**1.57**	**0.05**	**4.65**	**0.19**	**43.52**	**1.69**	**5.16**	**0.18**	**0.21**	**0.06**	**0.46**
H4 part 2	0.61	0.01	1.24	0.33	39.88	1.08	10.39	0.07	0.00	0.19	0.17
H4 part 2	1.12	0.00	1.07	0.24	43.44	0.96	9.41	0.09	0.20	0.19	0.23
H4 part 2	0.98	0.03	1.38	0.11	42.21	1.17	9.58	0.17	0.13	0.02	0.44
H4 part 2	0.98	0.17	1.03	0.25	37.27	1.69	15.47	0.17	0.00	0.13	0.43
H4 part 2 average (dark, coarse)	**0.92**	**0.05**	**1.18**	**0.23**	**40.70**	**1.23**	**11.21**	**0.13**	**0.08**	**0.13**	**0.32**
H4 part 3	0.20	0.00	0.30	0.17	11.25	1.43	39.85	0.00	0.00	0.00	0.00
H4 part 3	0.10	0.00	0.14	0.23	11.10	1.18	39.72	0.00	0.00	0.00	0.00
H4 part 3	0.33	0.00	0.00	0.17	10.74	1.34	40.29	0.00	0.21	0.00	0.00
H4 part 3	0.04	0.13	0.00	0.23	11.73	1.04	39.71	0.00	0.00	0.01	0.00
H4 part 3 average (vein)	**0.17**	**0.03**	**0.11**	**0.20**	**11.21**	**1.25**	**39.89**	**0.00**	**0.05**	**0.00**	**0.00**

*The average composition of the varicolored parts of concretions are summarized by the average compositions (bold)

4.3. Texture revealed by cathodoluminescence microscopy

Compared to normal light CL reveals some additional textural details: samples showed dull and bright orange luminescence under electron beam in the form of veinlet, layers and infiltration-like textures. The veinlet in sample H4 is zoned, its rim shows strong orange Mn^{2+} emission, but detailed electron microprobe study showed only little difference (~1 wt. %) in Mn content between the rim and the internal part of the vein. The CL spectra made on orange luminescent areas indicate a Mn^{2+}-activated emission in kutnohorite (Polgári et al., 2007). Non-luminescent areas are made of rhodochrosite.

4.4. TEM study

A microsample from the kutnohorite veinlet of sample H4 was investigated by TEM to determine its structural characteristics (Polgári et al., 2007). During analysis needle-like minerals in the form of single fibers, thick sheaves or mish-mash occurrences were also detected in the kutnohorite. Preliminary results on morphology and chemical composition indicate that these are chrysotile needles. It is very sensitive for radiation and contains a few atomic % Fe.

4.5. Stable C and O isotope study

18 concretions were analyzed on bulk samples. The values range between -19.43 and -8.38‰ $\delta^{13}C_{PDB}$, the average is -12.4‰ $\delta^{13}C_{PDB}$. In two concretions the core and the marginal part was separated and for the core -10.95 and -15.56 $\delta^{13}C_{PDB}$, while for the marginal part less negative values, -9.19 and -9.13 $\delta^{13}C_{PDB}$ were determined.

"Fish ball" H4 was analyzed in more detail.

From the core (fish fossil) to marginal parts of the concretion on the left, right, back and front side to up and down of the different colour (dark-core, medium and light-marginal part) parts were measured for C isotope distribution (Fig. 3). The most negative values occur in the core (-20.5 $\delta^{13}C_{PDB}$) around the fish fossil and radially toward the marginal part the values increase up to (-11.5 $\delta^{13}C_{PDB}$). The stable O isotope data of the 18 concretions range from -3.3 to +1.3‰ $\delta^{18}O_{PDB}$ (27.5 to 32.3‰ $\delta^{18}O_{SMOW}$).

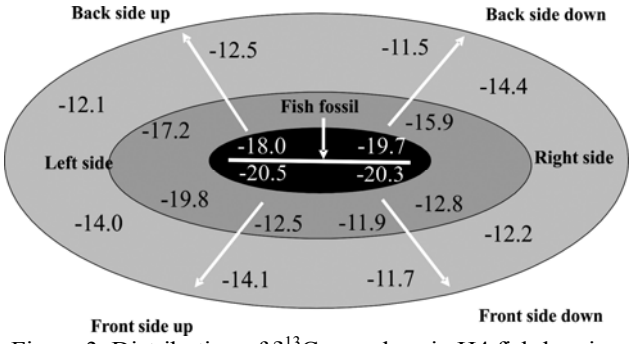

Figure 3. Distribution of $\delta^{13}C_{PDB}$ values in H4 fish-bearing concretion.

5. DISCUSSION

The main mineral composition of the concretions are rhodochrosite, Mn-bearing calcite, and Ca-rich kutnohorite, but the separation of these fine-grained minerals is not possible by routine polarizing microscope. However, these minerals can be distinguished easily on their cathodoluminescent characteristics: kutnohorite shows bright to dull orange luminescence (Polgári et al., 2007). Its textural features showing vein fillings and infiltrations of the matrix material of the concretions clearly reflect a later diagenetic formation of kutnohorite, after the formation of concretions.

Nothing shows elevated temperatures of the investigated diagenized sedimentary system, but the presence of kutnohorite is debate from this point of view. Recently, Kim et al., (2009) published experimental results of oxygen isotope fractionation between rhodochrosite and water at low temperatures and proposed new temperature-dependent relations between 10 and 40°C. Applying the equations of Kim et al., (2009) to our concretions and assuming an oxygen isotope value of −5‰ as proposed for Jurassic marine seawater (Veizer & Hoefs, 1976), yield partly negative temperatures. Assuming an oxygen isotope value of 0‰ for contemporaneous seawater gives more reasonable temperature estimates. Taking into consideration the results of these new calculations, the concretions at Úrkút Mn deposit probably formed under a temperature range of between 14.5 and 38°C. For the Úrkút Mn-carbonate deposit 13.4 and 27.0°C temperature range was published and the new results fit well with these estimated temperature conditions (Polgári et al., 2012).

Böttcher (2006) reported, that investigating the rhodochrosite-calcite solid-solution aqueous-solution system at low temperature the role of a dolomite-type ordered intermediate, kutnohorite, which is found only in natural high-temperature environments, has not been observed at low temperatures in sediments or experiments. On the other hand publications on sedimentary manganese mineralizations often report kutnohorite as a rare mineralogical component in these formations. Kutnohorite, a common member of the dolomite group, (general formula $CaMn(CO_3)_2$ is often cited as Mn-rich carbonate occurring as rare mineral in hydrothermal, metamorphosed and sedimentary sequences determined by XRD (Ozturk & Frakes, 1995; Gutzmer & Beukes 1996, 1998; Fan et al,. 1999; Hein et al., 1999; Krajewsky et al., 2001; Large et al., 2001; Burke & Kemp, 2002; Nyame et al., 2003). However, the chemical and structural characteristics of kutnohorite are rarely published. Vassileva et al., (2003 and references therein) review the detailed mineralogical and thermodynamic studies of kutnohorite, and Polgári et al., (2007) report chemical (EPMA) and structural (TEM) data and cathodoluminescence characterization of this Mn-rich carbonate. According to Böttcher (2006) on the basis of experimental studies, the stability and reactivity of ordered kutnohorite show that despite the thermodynamic stability field of the mineral, its formation at low temperatures seems to be kinetically inhibited.

TEM studies determined chrysotile in the kutnohorite-bearing concretions for the first time from Úrkút. Occurrence of chrysotile, a serpentine mineral, in a sedimentary system is unusual. It is known that chrysotile can rarely be formed by the hot-temperature silicification of dolomite phases. Fehér & Papp (2003) reported short chrysotile tubes in veinlets found in limestone at Szár Hill (Hungary). They supposed that Mg liberated during contact metamorphism of dolomite (or Mg-limestone). Mg was transported and deposited as brucite with calcite, and later the effect of siliceous hydrothermal fluids converted it to serpentine-bearing calcite veins.

In the case of the studied samples, silicification took place and double carbonate formation was characteristic during ore mineralization and later during diagenetic processes as well. Mg-excess also characterized the deposit, which partly could form chrysotile, and partly binded to carbonate minerals during diagenesis. The Ca content shares in phosphate

and carbonates. Intense silification also took place. It can explain the existence of chrysotile in the kutnohorite veinlet, but the hot-temperature conditions are not supported by the features of the unmetamorphosed deposit (oxygen isotope and mineralogical studies, Polgári et al., 2000, 2012). Stable O isotope results also support low-T formation conditions.

Organic remnant-bearing (fish or plant fragments) rhodochrosite-kutnohorite balls are common in the Úrkút manganese carbonate deposit. Similar, but mineralogically different calcareous concretions (dolomite balls or „coal balls") are well known from numerous coal formations (Deelman, 2003). The decomposition of organic remnants (plants, fish) have an important role in concretion formation in submarine environment. Algae might have withdrawn dissolved carbon dioxide from the shallow water, but decaying plant remains almost certainly relased carbon dioxide and thus led to the dissolution of any carbonates present. In the balls an excellent conservation of fish fossils can be seen. Only via quick petrification by calcium carbonate or by rhodochrosite the fossils were saved from decay. The carbonate must have precipitated from aqueous solution at a moment preceding burial. The in situ formation of the studied rhodochrositic fish balls took place just after burial in organic-rich (bacterioplankton) environment via bacterially-mediated Mn and sulphate reduction and organic matter decomposition and Mn-rich carbonate formation took place with phosphate formation and silicification as well. This process is well established by the $\delta^{13}C_{PDB}$ data, which in general are negative with a - 12.4‰ $\delta^{13}C_{PDB}$, on average of bulk of concretions. The detailed study around the fish fossil showed much more negative values near the organic remnant (strong central effect) with a increasing values toward the marginal parts of the concretion. The P content of the organic remnant during decomposition built into phosphate (hydroxyl apatite) around the fossil according to chemistry and mineralogy.

In our case there was a Mn-ore environment with very strong Mn-bearing effect. Decomposition of fish fossil created a special environment for diagenetic bacterial activity which probably influenced and controlled concretion formation and element mobilization. The mineralization around the fossil prevented the fish fossils from further decomposition processes, therefore whole fish could "survive".

6. CONCLUSION

22 concretions, among them 4 concretions with fish fossils ("fish balls") from the Úrkút Manganese Mine consist mainly of Ca-rhodochrosite, Mn-bearing calcite and moderately Ca-rich kutnohorite and close to the fish fossils hydroxyl-apatite. The formation of the concretions took place just after the burial of the fish fossils in organic rich (bacterioplankton) environment via bacterially mediated Mn and sulphate reduction and organic matter decomposition. Stable C and O isotope data confirm these formation processes.

The samples show the signs of diagenetic silicification in the form of quartz-cristobalite impregnations and vein fillings.

The cathodoluminescence microscopy seems to be very useful in the study of texture and diagenetic features of the sedimentary Mn ores, as kutnohorite was visible at the first time in the manganese carbonate ore. The textural appearance of this mineral supports its later diagenetic origin.

A detailed TEM study determined chrysotile in the kutnohorite veinlets for the first time, which was probably formed by the silicification of Mg-bearing carbonate or clay phases during diagenetic processes. The hot-temperature formation conditions in the ore deposit are not supported by other characteristics of the sedimentary Mn mineralization (O isotope data and clay mineralogy, etc.). Our results raise the possibility of low-T diagenetic formation of kutnohorite and chrysotile in organic matter-rich environment of the Mn ore deposit.

ACKNOWLEDGEMENTS

The financial background of this work was ensured by the Hungarian Scientific Research Fund (OTKA) Grant No. K 68992.

REFERENCES

Böttcher, ME., 2006. *The rhodochrosite-calcite solid-solution aqueous-solution sytem at low temperatures*. Geophysical Research Abstracts 8, 10034.

Buggisch, W. & Krumm, S. 2005. *Palaeozoic cold seep carbonates from Europe and North Africa - An integrated isotopic and geochemical approach*. Facies 50, 556-583.

Burke, IT. & Kemp, A.E.S. 2002. *Microfabric analysis of Mn-carbonate laminae deposition and Mn-sulfide formation in the Gotland Deep, Baltic Sea*. Geochimica et Cosmochimica Acta 66,9, 1589-1600.

Deelman, J.C. 2003. *Low-temperature formation of dolomite and magnesite*. Chapter 2, 25-65. Eindhoven, The Netherlands: Compact Disc Publications

El A., Cloutier, R. & Candilier, AM. 2002. *Early diagenesis of the Upper Devonian Escuminac Formation in the Gaspé Peninsula, Quebec: Sedimentological and geochemical evidence*. Sedimentary Geology, 146, 2-3, 209-223.

Fan, D., Hein, JR. & Ye, J., 1999. *Ordovician reef-hosted Jiaodingshan Mn-Co deposit and Dawashan Mn*

deposit, Sichuan Province, China. Ore Geology Reviews 15,1-3, 135-151.

Fara, E., Saraiva, AÁF., Campos, DDA., Moreira, JKR., Siebra, DDC. & Kellner, AWA. 2005. *Controlled excavations in the Romualdo Member of the Santana Formation (Early Cretaceous, Araripe Basin, northeastern Brazil): Stratigraphic, palaeoenvironmental and palaeoecological implications.* Palaeogeography, Palaeoclimatology, Palaeoecology, 218,1-2, 145-160.

Fehér, B. & Papp, G., 2003. *Brucite- and serpentine-bearing hydrothermal veinlets in the contact metamorphosed limestone of the Szár Hill, Polgárdi, Hungary.* Topographia Mineralogica Hungariae VIII, 135-144. (In Hungarian with English abstract)

Gutzmer, J. & Beukes, NJ. 1996. *Mineral paragenesis of the Kalahari manganese field, South Africa*. Ore Geology Reviews 11,6, 405-428.

Gutzmer, J. & Beukes, NJ. 1998. *The manganese formation of the Neoproterozoic Pengana Group, India, revision of an enigma.* Economic Geology, 93/7, 1091-1102.

Hein, JR., Fan, D., Ye, J., Liu, T. & Yeh, HW. 1999. *Composition and origin of Early Cambrian Tiantaishan phosphorite-Mn-carbonate ores, Shaanxi Province, China*. In: J.R. Hein, D. Fan (Eds.): Manganese and Assoicated Ore Deposits of China. Ore Geology Reviews 15, 95-134.

Kázmér, M. & Kovács, S. 1985. *Permian-Paleogene paleogeography along the eastern part of the Insubric-Periadriatic Lineament system: evidence for continental escape of the Bakony-Drauzug Unit.* Acta Geologica Hungarica, 28/1-2, 71-84.

Kim, ST., Kang, JO., Yun, ST., O'Neil, JR. & Mucci, A. 2009. *Experimental studies of oxygen isotope fractionation between rhodochrosite ($MnCO_3$) and water at low temperatures.* Geochimica Cosmochimca Acta 73/15, 4400-4408.

Krajewsky, KP., Lefeld, J. & Lacka, B. 2001. *Early diagenetic process in the formation of carbonate-hosted Mn ore deposit (Lower Jurassic, Tatra Mountains) as indicated from its carbon isotopic record*. Bulletin of the Polish Academy of Sciences Earth Sciences 49,1, 13-29.

Large, RR., Allen, RL., Blake, MD. & Herrmann, W. 2001. *Hydrothermal alteration and volatile element halos for the Rosebery K lens volcanic-hosted massive sulphide deposit, western Tasmania*. Economic Geology 96, 5, 1055-1072.

Lash, GG. & Blood D. 2004. *Geochemical and textural evidence for early (shallow) diagenetic growth of stratigraphically confined carbonate concretions, Upper Devonian Rhinestreet black shale, western New York.* Chemical Geology, 206,3-4, 407-424.

Nyame, FK., Beukes, NJ., Kase, K. & Yamamoto, M. 2003. *Compositional variations in manganese carbonate micronodules from the Lower Proterozoic Nsuta deposit, Ghana: Product of authigenic precipitation or postformational diagenesis?* Sedimentary Geology 154,3-4, 159-175.

Ozturk, H. & Frakes, LA. 1995. *Sedimentation and diagenesis of an Oligocene manganese deposit in a shallow subbasin of the Paratethys: Thrace Basin, Turkey*. Ore Geology Reviews 10,2, 117-132.

Pászti, A. 2004. *Fish fossils from the Úrkút Manganese Formation* (in Hungarian). Bányászati Kohászati Lapok Bányászat 137/6, 45-46.

Polgári, M., Okita, P.M. & Hein, J.R. 1991. *Stable isotope evidence for the origin of the Úrkút manganese ore deposit, Hungary*. Journal of Sedimentary Petrology 61,3, 384-393.

Polgári, M., Szabó, Z. & Szederkényi, T. (Eds.) 2000. *Manganese Ores in Hungary. In commemoration of professor Gyula Grasselly*. Szeged Regional Committee of the Hungarian Academy of Sciences, Juhász Publish House, Szeged, Hungary, 675 p.

Polgári, M., Philippe, M., Szabó-Drubina, M. & Tóth, M. 2005. *Manganese-impregnated wood from a Toarcian manganese ore deposit, Eplény Mine, Bakony Mts, Transdanubia, Hungary*. Neues Jahrbuch fur Geologie und Paläontologie - Monatshefte 3, 175-192.

Polgári, M., B., Bajnóczi, V., Kovács Kis, J., Götze, G., Dobosi, M., Tóth, T. & Vigh 2007. *Mineralogical and cathodoluminescence characteristics of Ca-rich kutnohorite from the Úrkút Mn-carbonate mineralization, Hungary*. Mineralogical Magazine, 71,5, 493-508.

Polgári, M., Hein, JR., Vigh, T., Szabó-Drubina, M., Fórizs, I., Bíró, L., Müller, A. & Tóth, L. 2012. *Microbial processes and the origin of the Úrkút manganese deposit, Hungary*. Ore Geology Reviews, 47, 87-109.

Tarawneh, K. & Moumani, K. 2006. *Petrography, chemistry and genesis of phosphorite concretions in the Eocene Umm Rijam Chert limestone Formation, Ma'an area, south, Jordan.* Journal of Asian Earth Sciences, 26/6, 627-635.

Vassileva, M., Dobrev, S. & Damyanov, Z. 2003. *Comparative characteristics of endogenic kutnohorite from Ribnitsa deposit and exogenic kutnohorite from Kremikovtsi deposit*. 50 years University of Mining and Geology "St. Ivan Rilski" Annual, vol. 46, Part I, Geology and Geophysics, Sofia, 195-200.

Veizer, J. & Hoefs, J. 1976. *The nature of O^{18}/O^{16} and C^{13}/C^{12} secular trends in sedimentary carbonate rocks.* Geochimica Cosmochimca Acta, 40, 1387-1395.

Vörös, A. & Galácz, A. 1998. *Jurassic palaeogeography of the Transdanubian Central Range (Hungary).* Riv. Ital. Paleontl. Strat., 104, 69-84.

Woo, KS. & Khim, BK. 2006. *Stable oxygen and carbon isotopes of carbonate concretions of the Miocene Yeonil Group in the Pohang Basin, Korea: Types of concretions and formation condition.* Sedimentary Geology, 183, 1-2, 15-30.

Receieved at: 11. 04. 2013
Revised at: 30. 09. 2013

Accepted for publication at: 04. 10. 2013
Published online at: 11. 10. 2013